Universal quantum gates between nitrogen-vacancy centers in a levitated nanodiamond

Xing-Yan Chen[1,2] and Zhang-qi Yin[1,*]

[1] *Center for Quantum Information, Institute for Interdisciplinary Information Sciences, Tsinghua University, Beijing 100084, China*
[2] *Max-Planck-Institut für Quantenoptik, Garching 85748, Germany*

(Dated: October 2, 2018)

We propose a scheme to realize universal quantum gates between nitrogen-vacancy (NV) centers in an optically trapped nanodiamond, through uniform magnetic field induced coupling between the NV centers and the torsional mode of the levitated nanodiamond. The gates are tolerant to the thermal noise of the torsional mode. By combining the scheme with dynamical decoupling technology, it is found that the high fidelity quantum gates are possible for the present experimental conditions. The proposed scheme is useful for NV-center-based quantum network and distributed quantum computation.

I. INTRODUCTION

Quantum computation is widely believed to be the core of the next generation of information technology. It could be used for solving problems that intractable for classical computers, such as prime factoring [1], quantum simulation [2], machining learning [3], optimization [4], etc. In order to realize practical quantum computation, many physical systems have been investigated, such trapped ions [5], superconducting qubits [6], nitrogen-vacancy(NV) centers in diamond [7, 8], etc. Compared with the other systems, the NV centers can perform quantum tasks, such as individually addressing and initialization, manipulation and detection in room temperature.

In the last decade, there are great progresses in NV centers based quantum information processing. In NV centers, the electron spins and the nearby nuclear spins couple with each other. The nuclear spins could be used as long time (> 1 s) quantum memory at room temperature [9]. By using geometric phase and optimizing the controlling pulses, the fault-tolerant universal quantum gates between the electron spins and the nuclear spins have been realized under ambient conditions [10, 11]. The error correction experiments have been performed in NV center by using both the electron and the nuclear spins, where phase errors have been corrected [12, 13]. To correct both phase-flip and bit-flip errors, at least five qubits need to be used, which is experimentally challenge.

The practical quantum computation needs not only fault tolerant, but also scalable. As proposed in Ref. [14–16], the scalable quantum computation in NV centers could be realized by connecting the small quantum registers with optical channels. The NV centers in distant diamonds have been entangled through interference and post selection of the emitted photons [17]. Using the similar method, the quantum teleportation [18], Bell inequality tests [19], entanglement distillation [20], and deterministic entanglement distribution [21] have been realized between the NV centers in distant diamond. Though quantum network based on the NV centers develops quickly, the small number of NV centers in every quantum node limits the computational ability of the whole network.

Up to now, in a single diamond two NV centers electron spins have been entangled through direct coupling [22]. In order to increase the number of NV centers in a single quantum register, many theoretical schemes have been proposed, such as the dark spin chain data bus [23, 24], cavity QED [25, 26], hybrid NV centers via superconducting circuits [27–29], etc. Recent years, there are more and more attentions on the approach of linking NV centers with mechanical resonators (phonons) [30–33]. It was found that by using magnetic field [34–37], or strain effects involving excited states [38], the strong coupling between the NV centers and the mechanical phonon modes could be realized. In these systems, the entanglement between multiple NV centers [39, 40], quantum simulation of many-body system [36], the single phonon source and detector [41, 42] and etc. have been investigated.

In this paper, we propose a scheme to realize controlled-phase gate using a levitated nanodiamond where qubits are represented by NV centers electron spins and the controlled-phase gate is mediated by torsional motion. The coupling between the electron spins and the torional mode is induced through the uniform external magnetic field [36, 37], which is relatively easy to realize compared to the schemes of $10^7 - 10^5$ T/m magnetic gradient induced strong coupling between translational motion and the NV center electron spin [34, 35]. Combining with the single qubit operations, we can achieve universal quantum computation in this system. Therefore, as a small universal quantum computer, the levitated nanodiamond with building-in NV centers could be a quantum node in a large quantum network, which could form a powerful distributed quantum computer. The two main decoherence effects: rethermalization of the mechanical motion and dephasing of NV centers have been analyzed both analytically and numerically.

* yinzhangqi@tsinghua.edu.cn

II. THE PROPOSED SETUP

We consider a non-spherical nanodiamond with one long axis and two short axes optically trapped in high vacuum in a static uniform magnetic field as shown in Fig.1(a). Two NV centers are placed at each side of the long axis and along different directions so that their magnetic field induced energy level shifts are different, thus allows single qubit addressing in the frequency domain. Here the qubits are represented by electron spins in the diamond NV centers and the spin-spin coupling is mediated by the librational mode of the nanodiamond. The distance of the two qubits is $d \sim 300$ nm in order to allow individual readout. Besides, as the coupling between the two NV centers scales with $1/d^3$ [43], in our setup it is in the order of Hz, much less than the spin-librational-mode coupling. Therefore, we neglect the direct coupling between NV centers in the Hamiltonian of the system.

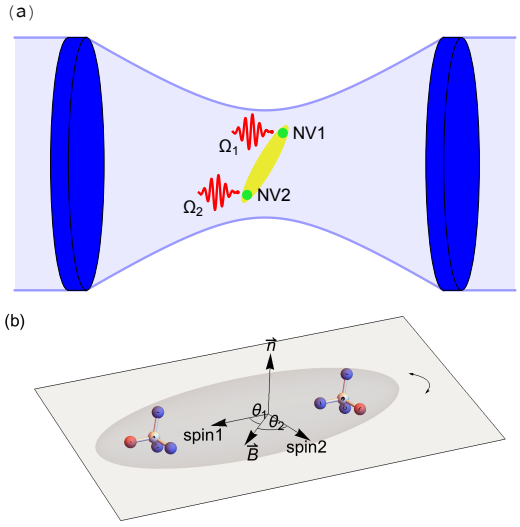

FIG. 1. (a) A nanodiamond with two NV centers placed at two endpoints of its long axis is optically trapped in vacuum with spin-torsional coupling through a static magnetic field. (b) Two NV centers in a levitated diamond nanocrystal in the presence of an uniform magnetic field. The rotation orientation $\vec{n}$ is perpendicular to NV centers' spin and the magnetic field $\vec{B}$. Torsional motion of the nanodiamond leads to change in angle θ which denotes the angle between the orientation of the NV center electron spin1 and $\vec{B}$.

We suppose that magnetic field $\vec{B}$ is homogeneous, and the angle between its direction and the direction of NV center electron spin1 θ changes with the torsional motion. In the energy basis of the NV centers, the total Hamiltonian for the two NV centers and the torsional oscillator reads

$$\begin{aligned} H &= \omega a^\dagger a + \frac{E(\theta_1)}{2}\sigma_1^z + \frac{E(\theta_2)}{2}\sigma_2^z + (g_1\sigma_1^z + g_2\sigma_2^z)(a + a^\dagger) \\ &= \omega a^\dagger a + \frac{\omega_1}{2}\sigma_1^z + \frac{\omega_2}{2}\sigma_2^z + \tilde{S}(a + a^\dagger), \end{aligned} \tag{1}$$

where $\hbar = 1$ (natural unit), $\tilde{S} = g_1\sigma_1^z + g_2\sigma_2^z$. ω is the angular frequency of the torsional mode, $E(\theta_i)$ $(i = 1, 2)$ is the energy splitting between $|s_z = 0\rangle_i \equiv |0\rangle_i$ and $|s_z = -1\rangle_i \equiv |1\rangle_i$ of the spin-1 eigenstates of the two NV centers at relative angle θ_i to the direction of the magnetic field. The coupling between the torsional mode and the NV center electron spin is

$$g_i = \sqrt{\frac{1}{8I\omega_i}}\frac{\partial E(\theta_i)}{\partial \theta_i}, \mathrm{i} = 1, 2, \tag{2}$$

where I is the moment of inertia of the nanodiamond.

In our proposal, the two NV centers are placed along two different directions of the four possible orientations, with an angle $\theta_1 + \theta_2 = 1.81$ rad, as shown in Fig.1(b). In general, the coupling strengths of the two NV centers g_1 and g_2 are different. In order to maximize the coupling strength, we control the torsional vibration direction to perpendicular to the two orientations of the NV centers and adjust the magnetic field to be parallel to the vibration plane, as illustrated in Fig.1(b). The value of g can be tuned in a wide range by controlling either the trap potential or the external magnetic field. We will show in the next section that the gate speed is determined by the effective coupling strength $g_{eff}^2/\omega = g_1 g_2/\omega$. As shown in Fig.2, the averaged coupling strength $g_{eff} = \sqrt{|g_1 g_2|}$ could be about $2\pi \times 25$ kHz at 0.05 T, which is much larger than the torsional mode decay ($<$ kHz), the NV center decay ($<$ kHz), and dephasing rates ($\sim$ kHz). It is comparable to other spin-phonon coupling strength with center of mass motion [30, 32, 35], where a large magnetic gradient $10^5 \sim 10^7$T/m is needed, while our scheme only requires a uniform magnetic field.

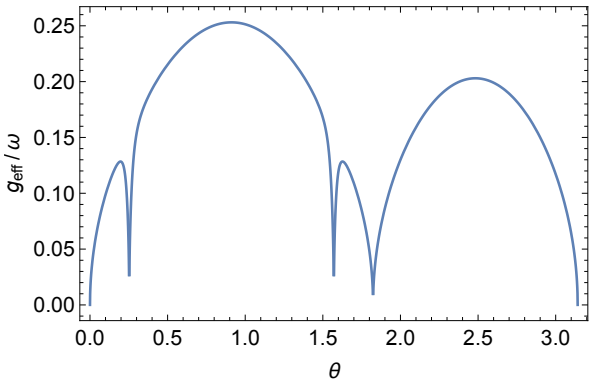

FIG. 2. An example of ratio between effective coupling strength $g_{eff} = \sqrt{|g_1 g_2|}$ and torsional frequency ω as a function of relative angle θ, with the magnetic field $B = 7$ mT and $\omega = 2\pi \times 0.1$ MHz. The torsional frequency ω is chosen to fulfill $g/\omega = 1/4$ at the maximum.

In principle, the nanodiamond can contain multiple NV centers which couple to the same torsional mode. The NV centers should be separated by more than 100 nm to suppress unwanted dipole-dipole interactions and support the individual readout [44]. Therefore in order to

embedding more NV centers, the size of the nanodiamond should increase, which would decrease the torsional frequency and reduce the coupling strength. The size effect on the coupling strength is shown in Fig.3. When the long and short axis are 300 nm and 200 nm, respectively, the number of the embedded NV can be about 10, and the electron spins torsional mode coupling g around $2\pi \times 20$ kHz.

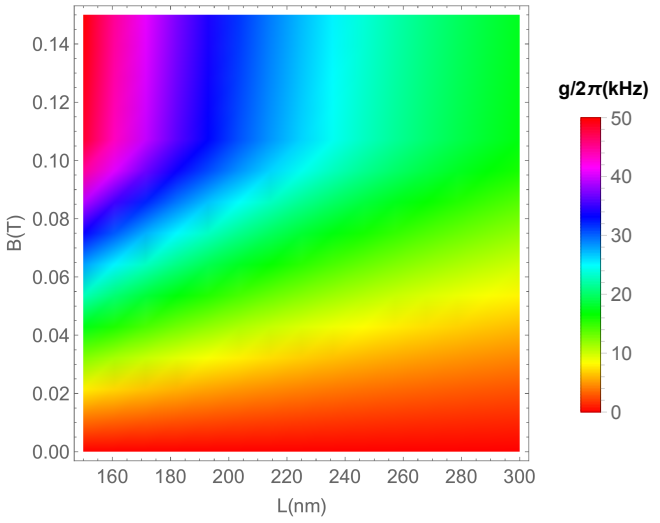

FIG. 3. The coupling strength g under different length L of the nanodiamond and the external magnetic field B. The ratio of the long and short axis is fixed to be 1.5. The torsional frequency is taken to be $2\pi \times 0.1$ MHz at $L = 150$ nm. The coupling strength is optimized along all the relative direction of the spin to the magnetic field, e.g. take the maximum value in Fig.2.

III. GATE OPERATION UNDER IDEAL CONDITIONS

Single qubit operations can be realized by simply adding microwave pulses to induce transition between the two energy levels which represent $|0\rangle$ and $|1\rangle$ with proper phase. If the Rabi frequency of the drive is large enough, we can ignore the term $g\sigma_z(a+a^\dagger)$ which brings about unwanted coupling to the vibration. Another way to decouple the qubit states from the resonator is to incorporate dynamical decoupling [45, 46] or geometric approach [10, 47] which simultaneously suppress the noise caused by a nuclear-spin bath. Further description and numerical simulation on noise effect will be presented in the section IV.

Here we propose a method to realize controlled phase gates and universal computation could be achieved when combined with single qubit operations. Our method is inspired by the celebrated Sørensen-Mølmer gates for hot trapped ions [48, 49] or similar bus-based quantum gates [30, 35, 50, 51]. In the interaction picture of $A = \frac{\omega_1}{2}\sigma_1^z + \frac{\omega_2}{2}\sigma_2^z$, we obtain the interaction Hamiltonian

$$\begin{aligned} H' &= \omega a^\dagger a + \tilde{S}(a + a^\dagger) \\ &= \omega(a + \frac{\tilde{S}}{\omega})^\dagger(a + \frac{\tilde{S}}{\omega}) - \frac{\tilde{S}^2}{\omega} \end{aligned} \tag{3}$$

Using similar method as [51], the Hamiltonian (3) can be rewritten as

$$H' = U[\omega a^\dagger a - \frac{\tilde{S}^2}{\omega}]U^\dagger, \tag{4}$$

where U is unitary transformation $U = \exp[\frac{\tilde{S}}{\omega}(a - a^\dagger)]$. The time evolution governed by the Hamiltonian (3) reads

$$e^{-iH't} = Ue^{-i\omega t a^\dagger a}e^{i\frac{\tilde{S}^2}{\omega}t}U^\dagger. \tag{5}$$

For certain times when $\omega t_m = 2\pi m$ with $m = 1, 2, 3\cdots$, the first exponential $e^{-i\omega t_m a^\dagger a} = \mathbb{1}$ since the number operator has an integer spectrum. Thus time evolution reduces to

$$e^{-iH't_m} = \exp\left[2i\pi m(\frac{\tilde{S}}{\omega})^2\right]. \tag{6}$$

Substituting $\tilde{S}^2 = g_1^2 + g_2^2 + 2g_1g_2\sigma_1^z \otimes \sigma_2^z$, and ignoring the unimportant global phase we get

$$e^{-iH't_m} = \exp(4i\pi m\frac{g_1g_2}{\omega^2}\sigma_1^z \otimes \sigma_2^z). \tag{7}$$

Returning to the laboratory frame, the full evolution is governed by $e^{-iH't_m}e^{-iAt_m}$. We now show that the e^{-iAt_m} term can be canceled exactly by the standard spin-echo technique, which compensates the unknown detuning as well. Denoting a global flip of all qubits around the axis $\alpha = x, y, z$ as $U_\alpha(\varphi) = exp(-i\varphi/2\Sigma_i\sigma_i^\alpha)$, the full evolution (in the basis $\{|00\rangle, |10\rangle, |01\rangle, |11\rangle\}$), intertwined by spin-echo pulses, reads as

$$U(2t_m) = U_x(\pi)e^{-iH't_m}e^{-iAt_m}U_x(\pi)e^{-iH't_m}e^{-iAt_m} \tag{8}$$

$$= \mathrm{diag}(e^{i\phi}, 1, 1, e^{i\phi}), \tag{9}$$

with $\phi = 8m\pi(g_{eff}/\omega)^2$ and $g_{eff} = \sqrt{|g_1g_2|}$. After complementing the propagator $U(2t_m)$ with $U_z(-\phi)$, we obtain

$$U_{\mathrm{Cphase}} = U_z(-\phi)U(2t_m) \tag{10}$$

$$= \mathrm{diag}(1, 1, 1, e^{2i\phi}) \tag{11}$$

which is a controlled phase gate for $\phi = \pi/2$, corresponding to a gate time $t_{max} = 2t_m = 4\pi m/\omega = \pi/4g_{eff}$. Here m must take integer value. The condition $\phi = \pi/2$ can be archieved when

$$g_{eff}/\omega = \frac{1}{4\sqrt{m}}. \tag{12}$$

which gives $g_{eff}/\omega = 1/4$ for $m = 1$. To fulfill the above condition we can change ω by tuning the power and waist of the optical tweezer. As an example, in Fig. 2, for given magnetic field, we can choose appropriate ω to approximate condition Eq.(12) with $m = 1$ in a wide range (from 0.8 to 1.0 rad) of direction θ.

IV. DECOHERENCE EFFECT

The main sources of decoherence in this hybrid system of solid-state spins and mechanical oscillator are the rethermalization of the torsional mode towards equilibrium thermal occupation and the dephasing effect of the spins. The dissipative dynamics under these decoherence effects can be described by the master equation for the system's density matrix ρ,

$$\dot{\rho} = -i[H,\rho] + \kappa(\bar{n}_{th}+1)\mathcal{D}[a]\rho + \kappa\bar{n}_{th}\mathcal{D}[a^\dagger]\rho + \frac{\Gamma}{4}\sum_{i=1,2}\mathcal{D}[\sigma_i^z]\rho \quad (13)$$

with $\mathcal{D}[a]\rho = a\rho a^\dagger - \frac{1}{2}\{a^\dagger a, \rho\}$ and the torsional mode decay rate $\kappa = \omega/Q$, where Q is the quality factor of the torsional mode. The second and the third terms in Eq. (13) describe the rethermalization of the torsional mode towards the thermal occupation $\bar{n}_{th} = [\exp(\hbar\omega/k_BT)-1]^{-1}$ at temperature T. The last term in Eq. (13) describes the dephasing of the qubits with a dephasing rate $\Gamma \sim 1/T_2$, where T_2 is the time-averaged dephasing time. Here we have ignored single-spin relaxation processes as the associated time scale T_1 is typically much longer than T_2. Nevertheless, by using dynamically decoupling techniques [46, 52–54] the coherence time can be efficiently prolong to approach T_1.

In the case of single qubit gates, the coupling between the mechanical mode and the spin $g\sigma_i^z(a+a^\dagger)$ serves as an extra dephasing channel. The coupling induced dephasing effect, characterized by δ_g, grows with the thermal occupation $\bar{n}_{th}$, and is much larger than the effect of nuclear-spin bath δ_S under typical experimental parameters $\bar{n}_{th} \sim 1\times10^3$. Therefore, in the following section we introduce a dynamical corrected operation which can significantly reduce both dephasing effects.

A. single qubit gates

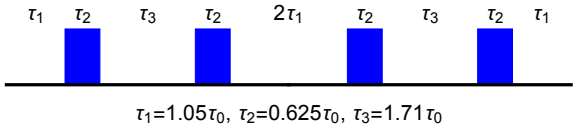

FIG. 4. Pulse sequences of 5-piece SUPCODE sequences [52]. The time duration $\tau_0 = (2+\theta/2\pi)t_0$ for a θ rotation pulse.

For single qubit operations, we consider an on-resonance drive along x axis with Rabi frequency ($\Omega \sim 2\pi \times 50$ MHz. The Hamiltonian can be written as $H = 2\pi(\delta S_z + \Omega S_x)$, with $\delta = \delta_S + \delta_g$ represents the effect of interaction with the nuclear-spin bath and coupling to the mechanical motion. The hyperfine interaction with the nuclear spin results in a random local magnetic field $\delta_S = \Sigma_k b_k I_z^k$ of typical strength of the order of magnitude of about 1 MHz in solids. The coupling effect of the mechanical mode can be estimated by $\delta_g = g(a+a^\dagger) \sim 2g\sqrt{\bar{n}_{th}}$ for $\bar{n}_{th} \gg 1$. With a five-piece SUPCODE pulse described in [52], the infidelity of the π gate can be estimated by $64.1(\delta/\Omega)^6 + O(\delta/\Omega)^8$. The 5-piece pulse sequence is shown in Fig.4.

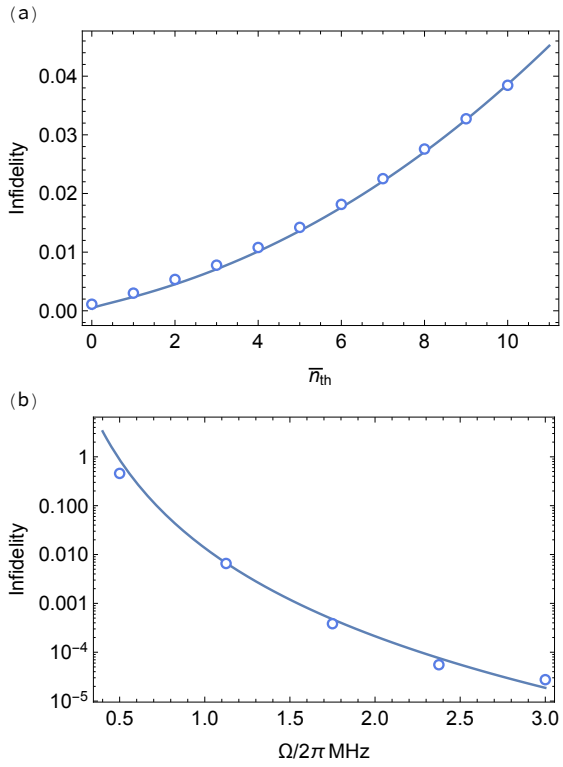

FIG. 5. Infidelity due to coupling to torsional mode as a function of (a) thermal occupation $\bar{n}_{th}$ with Rabi frequency $\Omega = 2\pi\times1$ MHz; (b) Rabi frequency Ω, with thermal occupation $\bar{n}_{th} = 5$. The torsional frequency $\omega = 2\pi\times0.1$ MHz and coupling strength $g = \omega/4$. Blue circles are numerical results obtained by solving the master equationn, and the blue line is the fitted model of Eq.(14) with $n_0 = 2.65$.

In the following, we provide the numerical results of the master equation Eq.(13), for the five-piece SUPCODE π pulse around x(y) axis. For thermal occupation $\bar{n}_{th} = 1000$, the dephasing induced by coupling to the resonator mode $\delta_g \sim 4$MHz while the typical strength of the random magnetic field $\delta_S \sim 1$ MHz. We focus on the coupling effect here, and leave the discussion of rethermalization and dephasing in the next section. Typical results from our numerical simulations are displayed in

Fig.5. The results can be well explained by a fit to

$$\xi = 1 - \mathcal{F} = 64.1(\frac{2g(\sqrt{\bar{n}_{th}} + n_0)}{\Omega})^6, \qquad (14)$$

which is obtained by replace $g(a+a^\dagger)$ by $2g(\sqrt{\bar{n}_{th}}+n_0)$ in the noise parameter δ. The parameter n_0 represents the thermal fluctuation which still exists at thermal vacuum.

By Eq.(14), even with large thermal occupation $\bar{n}_{th} = 300$, infidelity $\sim 10^{-3}$ can be achieved with Rabi frequency $\Omega \sim 2\pi \times 10\,\mathrm{MHz}$.

B. controlled phase gate

For controlled phase gate, we provide numerical results of the master equation (13), for the initial product state $\rho(0) = (|00\rangle + |11\rangle)(\langle 00| + \langle 11|) \otimes \rho_{th}(T)$. We quantify the state fidelity $\mathcal{F} = \langle \Phi_{tar}|\varrho|\Phi_{tar}\rangle$ with the target state $|\Phi_{tar}\rangle = (|00\rangle - |11\rangle)/\sqrt{2}$; here, $\varrho = tr_a[\rho]$ refers to the density matrix of the qubits, with $tr_a[...]$ denoting the trace over the resonator degrees of freedom. Here we use dynamical decoupling pulse described in [55, 56] which can suppress the decoherence rate Γ by two or three orders of magnitude as compared with the pure dephasing rate. In order to study the individual effects of the decoherence channel, we treat them separately here, and assume perfect single qubit operation. This separate treatment is justified by comparing the sum of individual errors with the results from full master equation. Typical results from our numerical simulations are displayed in Fig.6. For small infidelities ($g_{\text{eff}} \gg k_{\text{eff}}, \Gamma$), the individual linear error terms due to cavity rethermalization and qubit dephasing can be added independently. Using the simple linear error model in [51], the total error reads

$$\xi \approx \alpha_\kappa/Q\bar{n}_{th} + \alpha_\Gamma\Gamma/\omega. \qquad (15)$$

Based on results in Fig. 6 we extract the coefficient $\alpha_\kappa \approx 4$ and $\alpha_\Gamma \approx 0.2(\omega/g_{eff})^2$. Here the coefficient related to dephasing α_Γ is different from the result in [51] by a factor of 2, as the controlled-phase gate time in our proposal is twice as the time as it is to obtain the maximally entangled state. We can estimate an upper limit of the thermal occupation number $n_t h$ with typical parameters in our system are $\omega = 2\pi \times 1\,\mathrm{MHz}$, $g/\omega = 1/4$. For a high Q torsional mode with $Q = 10^{11}$, the rethermalization effect can be ignored even at room temperature(corresponding to $\bar{n}_{th} \approx 8 \times 10^6$) . Nevertheless, in order to avoid an-harmonic effect of large torsional amplitude $\Delta\theta$, the condition $\frac{1}{2}\partial^2 E/\partial\theta^2(\Delta\theta)^2 \ll \partial E/\partial\theta\Delta\theta$ has to be fulfilled which corresponding to $\bar{n}_{th} \ll 3 \times 10^6$. In addition to rethermalization, the effective dephasing rate given a pure dephasing rate 100kHz is 1kHz [46, 54], which gives the estimated error $\xi \approx 0.3\%$.

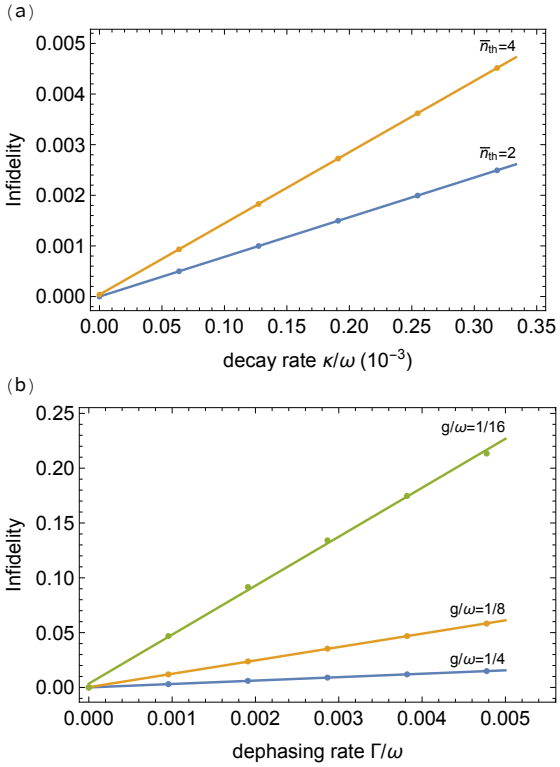

FIG. 6. Errors ($\xi = 1 - \mathcal{F}_{max}$) due to rethermalization of the cavity mode (a) and qubit dephasing (b). (a) Rethermalization-induced error for $\bar{n}_{th} = 2$ (blue) and $\bar{n}_{th} = 4$ (orange), and $\Gamma = 0$. (b) Dephasing-induced errors for $\mu = g/\omega = 1/4$ (blue), $\mu = 1/8$(orange), and $\mu = 1/16$ (green); here, $\kappa/\omega = 10^{-6}$ and $\bar{n}_{th} = 0.01$. In both cases, the linear error scaling is verified.

V. CONCLUSIONS

We have proposed a scheme to realize a high-fidelity universl quantum gates in a spin-torsional motion system, even in the presence of a thermally populated torsional mode. Our proposal uses a uniform magnetic field instead of a large magnetic gradient and thus reduce the noise caused by fluctuation of magnetic field. The spin-torsional coupling can be larger than 100 kHz which allows a short gate time less than 8 μs for a controlled-phase gate. The two main decoherence effects: rethermalization of the mechanical motion and dephasing of NVs have been analyzed both analytically and numerically. The mechanical motion serves as the quantum bus for two qubit controlled-phase gates while induces extra dephasing channel for single qubit gates. To increase the coherence time, we have incorporated dynamical decoupling method for single qubit gates. It is found that the high fiedlity larger than 99% universal quantum gates are possible under the current experimental conditions. Our scheme could be applied for distributed quantum computation and quantum network based on NV centers.

ACKNOWLEDGMENTS

This work is supported by National Natural Science Foundation of China NO. 61771278, 61435007, and the Joint Foundation of Ministry of Education of China (6141A02011604). We thank the helpful discussions with Tongcang Li.

[1] Andrew M. Childs and Wim van Dam, "Quantum algorithms for algebraic problems," Rev. Mod. Phys. **82**, 1–52 (2010).

[2] I. M. Georgescu, S. Ashhab, and Franco Nori, "Quantum simulation," Rev. Mod. Phys. **86**, 153–185 (2014).

[3] J. Biamonte, P. Wittek, N. Pancotti, P. Rebentrost, N. Wiebe, and S. Lloyd, "Quantum machine learning," Nature (London) **549**, 195–202 (2017).

[4] E. Farhi, J. Goldstone, and S. Gutmann, "A Quantum Approximate Optimization Algorithm," ArXiv e-prints (2014), arXiv:1411.4028 [quant-ph].

[5] H. Häffner, C. F. Roos, and R. Blatt, "Quantum computing with trapped ions," Phys. Rep. **469**, 155 (2008).

[6] Alexandre Blais, Ren-Shou Huang, Andreas Wallraff, S. M. Girvin, and R. J. Schoelkopf, "Cavity quantum electrodynamics for superconducting electrical circuits: An architecture for quantum computation," Phys. Rev. A **69**, 062320 (2004).

[7] M. W. Doherty, N. B. Manson, P. Delaney, F. Jelezko, J. Wrachtrup, and L. C. L. Hollenberg, "The nitrogen-vacancy colour centre in diamond," Phys. Rep. **528**, 1–45 (2013).

[8] Gang-Qin Liu and Xin-Yu Pan, "Quantum information processing with nitrogen-vacancy centers in diamond," Chinese Physics B **27**, 020304 (2018).

[9] P. C. Maurer, G. Kucsko, C. Latta, L. Jiang, N. Y. Yao, S. D. Bennett, F. Pastawski, D. Hunger, N. Chisholm, M. Markham, D. J. Twitchen, J. I. Cirac, and M. D. Lukin, "Room-Temperature Quantum Bit Memory Exceeding One Second," Science **336**, 1283 (2012).

[10] C. Zu, W.-B. Wang, L. He, W.-G. Zhang, C.-Y. Dai, F. Wang, and L.-M. Duan, "Experimental realization of universal geometric quantum gates with solid-state spins," Nature **514**, 72 (2014).

[11] X. Rong, J. Geng, F. Shi, Y. Liu, K. Xu, W. Ma, F. Kong, Z. Jiang, Y. Wu, and J. Du, "Experimental fault-tolerant universal quantum gates with solid-state spins under ambient conditions," Nature Communications **6**, 8748 (2015).

[12] G. Waldherr, Y. Wang, S. Zaiser, M. Jamali, T. Schulte-Herbrüggen, H. Abe, T. Ohshima, J. Isoya, J. F. Du, P. Neumann, and J. Wrachtrup, "Quantum error correction in a solid-state hybrid spin register," Nature (London) **506**, 204 (2014).

[13] T. H. Taminiau, J. Cramer, T. van der Sar, V. V. Dobrovitski, and R. Hanson, "Universal control and error correction in multi-qubit spin registers in diamond," Nature Nanotechnology **9**, 171–176 (2014), arXiv:1309.5452 [cond-mat.mes-hall].

[14] Liang Jiang, Jacob M. Taylor, Anders S. Sørensen, and Mikhail D. Lukin, "Distributed quantum computation based on small quantum registers," Phys. Rev. A **76**, 062323 (2007).

[15] Kae Nemoto, Michael Trupke, Simon J. Devitt, Ashley M. Stephens, Burkhard Scharfenberger, Kathrin Buczak, Tobias Nöbauer, Mark S. Everitt, Jörg Schmiedmayer, and William J. Munro, "Photonic architecture for scalable quantum information processing in diamond," Phys. Rev. X **4**, 031022 (2014).

[16] C. Monroe, R. Raussendorf, A. Ruthven, K. R. Brown, P. Maunz, L.-M. Duan, and J. Kim, "Large-scale modular quantum-computer architecture with atomic memory and photonic interconnects," Phys. Rev. A **89**, 022317 (2014).

[17] H. Bernien, B. Hensen, W. Pfaff, G. Koolstra, M. S. Blok, L. Robledo, T. H. Taminiau, M. Markham, D. J. Twitchen, L. Childress, and R. Hanson, "Heralded entanglement between solid-state qubits separated by three metres," Nature **497**, 86 (2013).

[18] W. Pfaff, B. J. Hensen, H. Bernien, S. B. van Dam, M. S. Blok, T. H. Taminiau, M. J. Tiggelman, R. N. Schouten, M. Markham, D. J. Twitchen, and R. Hanson, "Unconditional quantum teleportation between distant solid-state quantum bits," Science **345**, 532 (2014).

[19] B. Hensen, H. Bernien, A. E. Dréau, A. Reiserer, N. Kalb, M. S. Blok, J. Ruitenberg, R. F. L. Vermeulen, R. N. Schouten, C. Abellán, W. Amaya, V. Pruneri, M. W. Mitchell, M. Markham, D. J. Twitchen, D. Elkouss, S. Wehner, T. H. Taminiau, and R. Hanson, "Loophole-free Bell inequality violation using electron spins separated by 1.3 kilometres," Nature (London) **526**, 682 (2015).

[20] N. Kalb, A. A. Reiserer, P. C. Humphreys, J. J. W. Bakermans, S. J. Kamerling, N. H. Nickerson, S. C. Benjamin, D. J. Twitchen, M. Markham, and R. Hanson, "Entanglement distillation between solid-state quantum network nodes," Science **356**, 928 (2017).

[21] P. C. Humphreys, N. Kalb, J. P. J. Morits, R. N. Schouten, R. F. L. Vermeulen, D. J. Twitchen, M. Markham, and R. Hanson, "Deterministic delivery of remote entanglement on a quantum network," Nature **558**, 268 (2018).

[22] F. Dolde, I. Jakobi, B. Naydenov, N. Zhao, S. Pezzagna, C. Trautmann, J. Meijer, P. Neumann, F. Jelezko, and J. Wrachtrup, "Room-temperature entanglement between single defect spins in diamond," Nature Physics **9**, 139–143 (2013).

[23] N. Y. Yao, L. Jiang, A. V. Gorshkov, P. C. Maurer, G. Giedke, J. I. Cirac, and M. D. Lukin, "Scalable architecture for a room temperature solid-state quantum information processor," Nature Communications **3**, 800 (2012).

[24] N. Y. Yao, Z.-X. Gong, C. R. Laumann, S. D. Bennett, L.-M. Duan, M. D. Lukin, L. Jiang, and A. V. Gor-

shkov, "Quantum logic between remote quantum registers," Phys. Rev. A **87**, 022306 (2013).
[25] Y.-S. Park, A. K. Cook, and H. Wang, "Cavity QED with Diamond Nanocrystals and Silica Microspheres," Nano Letters **6**, 2075–2079 (2006), cond-mat/0608493.
[26] W. L. Yang, Z. Q. Yin, Z. Y. Xu, M. Feng, and J. F. Du, "One-step implementation of multiqubit conditional phase gating with nitrogen-vacancy centers coupled to a high-Q silica microsphere cavity," Applied Physics Letters **96**, 241113 (2010).
[27] Y. Kubo, F. R. Ong, P. Bertet, D. Vion, V. Jacques, D. Zheng, A. Dréau, J.-F. Roch, A. Auffeves, F. Jelezko, J. Wrachtrup, M. F. Barthe, P. Bergonzo, and D. Esteve, "Strong coupling of a spin ensemble to a superconducting resonator," Phys. Rev. Lett. **105**, 140502 (2010).
[28] D. Marcos, M. Wubs, J. M. Taylor, R. Aguado, M. D. Lukin, and A. S. Sørensen, "Coupling nitrogen-vacancy centers in diamond to superconducting flux qubits," Phys. Rev. Lett. **105**, 210501 (2010).
[29] W. L. Yang, Z. Q. Yin, Y. Hu, M. Feng, and J. F. Du, "High-fidelity quantum memory using nitrogen-vacancy center ensemble for hybrid quantum computation," Phys. Rev. A **84**, 010301 (2011).
[30] P. Rabl, S. J. Kolkowitz, F. H.L. Koppens, J. G.E. Harris, P. Zoller, and M. D. Lukin, "A quantum spin transducer based on nanoelectromechanical resonator arrays," Nat. Phys. **6**, 602 (2010).
[31] S. D. Bennett, N. Y. Yao, J. Otterbach, P. Zoller, P. Rabl, and M. D. Lukin, "Phonon-Induced Spin-Spin Interactions in Diamond Nanostructures: Application to Spin Squeezing," Phys. Rev. Lett. **110**, 156402 (2013).
[32] Z. Yin, N. Zhao, and T. Li, "Hybrid opto-mechanical systems with nitrogen-vacancy centers," Science China Physics, Mechanics, and Astronomy **58**, 050303 (2015).
[33] M. C. Kuzyk and H. Wang, "Phononic Quantum Networks of Solid-State Spins with Alternating and Frequency-Selective Waveguides," ArXiv e-prints (2018), arXiv:1804.07862 [quant-ph].
[34] P. Rabl, P. Cappellaro, M. V. Gurudev Dutt, L. Jiang, J. R. Maze, and M. D. Lukin, "Strong magnetic coupling between an electronic spin qubit and a mechanical resonator," Phys. Rev. B **79**, 041302 (2009).
[35] Zhang-qi Yin, Tongcang Li, Xiang Zhang, and L. M. Duan, "Large quantum superpositions of a levitated nanodiamond through spin-optomechanical coupling," Phys. Rev. A **88**, 033614 (2013).
[36] Yue Ma, Thai M. Hoang, Ming Gong, Tongcang Li, and Zhang-qi Yin, "Proposal for quantum many-body simulation and torsional matter-wave interferometry with a levitated nanodiamond," Phys. Rev. A **96**, 023827 (2017).
[37] T. Delord, L. Nicolas, Y. Chassagneux, and G. Hétet, "Strong coupling between a single nitrogen-vacancy spin and the rotational mode of diamonds levitating in an ion trap," Phys. Rev. A **96**, 063810 (2017).
[38] D. Andrew Golter, Thein Oo, Mayra Amezcua, Ignas Lekavicius, Kevin A. Stewart, and Hailin Wang, "Coupling a surface acoustic wave to an electron spin in diamond via a dark state," Phys. Rev. X **6**, 041060 (2016).
[39] Z. Y. Xu, Y. M. Hu, W. L. Yang, M. Feng, and J. F. Du, "Deterministically entangling distant nitrogen-vacancy centers by a nanomechanical cantilever," Phys. Rev. A **80**, 022335 (2009).
[40] L.-G. Zhou, L. F. Wei, M. Gao, and X.-B. Wang, "Strong coupling between two distant electronic spins via a nanomechanical resonator," Phys. Rev. A **81**, 042323 (2010).
[41] R.-X. Wang, K. Cai, Z.-Q. Yin, and G.-L. Long, "Quantum memory and non-demolition measurement of single phonon state with nitrogen-vacancy centers ensemble," Optics Express **25**, 30149 (2017), arXiv:1705.10954 [quant-ph].
[42] K. Cai, Z.-W. Pan, R.-X. Wang, D. Ruan, Z.-Q. Yin, and G.-L. Long, "Single phonon source based on a giant polariton nonlinear effect," Optics Letters **43**, 1163 (2018), arXiv:1711.06835 [quant-ph].
[43] A. Bermudez, F. Jelezko, M. B. Plenio, and A. Retzker, "Electron-mediated nuclear-spin interactions between distant nitrogen-vacancy centers," Phys. Rev. Lett. **107**, 150503 (2011).
[44] Huiliang Zhang, Keigo Arai, Chinmay Belthangady, J-C Jaskula, and Ronald L Walsworth, "Selective addressing of solid-state spins at the nanoscale via magnetic resonance frequency encoding," npj Quantum Information **3**, 31 (2017).
[45] Kaveh Khodjasteh, Daniel A. Lidar, and Lorenza Viola, "Arbitrarily Accurate Dynamical Control in Open Quantum Systems," Phys. Rev. Lett. **104**, 090501 (2010).
[46] I. Cohen, N. Aharon, and A. Retzker, "Continuous dynamical decoupling utilizing time-dependent detuning," Fortschritte der Phys. **65**, 1600071 (2017).
[47] Erik Sjöqvist, D. M. Tong, L. Mauritz Andersson, Björn Hessmo, Markus Johansson, and Kuldip Singh, "Non-adiabatic holonomic quantum computation," New J. Phys. **14**, 103035 (2012).
[48] Klaus Mølmer and Anders Sørensen, "Multiparticle Entanglement of Hot Trapped Ions," Phys. Rev. Lett. **82**, 1835 (1999).
[49] Anders Sørensen and Klaus Mølmer, "Entanglement and quantum computation with ions in thermal motion," Phys. Rev. A **62**, 022311 (2000).
[50] Shimon Kolkowitz, Ania C. Bleszynski Jayich, Quirin P. Unterreithmeier, Steven D. Bennett, Peter Rabl, J. G. E. Harris, and Mikhail D. Lukin, "Coherent Sensing of a Mechanical Resonator with a Single-Spin Qubit," Science **335**, 1603 (2012).
[51] M. J. A. Schuetz, G. Giedke, L. M. K. Vandersypen, and J. I. Cirac, "High-fidelity hot gates for generic spin-resonator systems," Phys. Rev. A **95**, 052335 (2017).
[52] Xing Rong, Jianpei Geng, Zixiang Wang, Qi Zhang, Chenyong Ju, Fazhan Shi, Chang-Kui Duan, and Jiangfeng Du, "Implementation of Dynamically Corrected Gates on a Single Electron Spin in Diamond," Phys. Rev. Lett. **112**, 050503 (2014).
[53] J-M Cai, B. Naydenov, R. Pfeiffer, L. P. McGuinness, K. D. Jahnke, F. Jelezko, M. B. Plenio, and A. Retzker, "Robust dynamical decoupling with concatenated continuous driving," New J. Phys. **14**, 113023 (2012).
[54] I. Cohen, T. Unden, F. Jelezko, and A. Retzker, "Protecting a nuclear spin from a noisy electron spin in diamond," ArXiv e-prints (2017), arXiv:1703.01596 [quant-ph].
[55] Jacob R. West, Daniel A. Lidar, Bryan H. Fong, and Mark F. Gyure, "High Fidelity Quantum Gates via Dynamical Decoupling," Phys. Rev. Lett. **105**, 230503 (2010).
[56] Hui Khoon Ng, Daniel A. Lidar, and John Preskill, "Combining dynamical decoupling with fault-tolerant quantum computation," Phys. Rev. A **84**, 012305 (2011).